Polarized Fluorescence of Aggregated Bacteriochlorophyll *c* and Baseplate Bacteriochlorophyll *a* in Single Chlorosomes Isolated from *Chloroflexus aurantiacus*†

Yutaka Shibata,*,‡ Yoshitaka Saga,§ Hitoshi Tamiaki,|| and Shigeru Itoh‡

Division of Material Science (Physics), Graduate School of Science, Nagoya University, Nagoya 464-8602, Japan, Department of Chemistry, Faculty of Science and Engineering, Kinki University, Higashi-Osaka, Osaka 577-8502, Japan, and Department of Bioscience and Biotechnology, Faculty of Science and Engineering, Ritsumeikan University, Kusatsu, Shiga 525-8577, Japan

Received November 8, 2006; Revised Manuscript Received April 12, 2007

ABSTRACT: The polarization anisotropy of fluorescence from single chlorosomes isolated from a green filamentous bacterium, *Chloroflexus aurantiacus*, was measured using a confocal laser microscope at 13 K. Each single chlorosome that is floating in a frozen solvent exhibited strong polarization anisotropy of fluorescence. We calculated the degrees of fluorescence polarization for 51 floating single chlorosomes. The value ranged from 0.1 to 0.76 for the BChl-*c* aggregate in the core chlorosomes and from 0 to 0.4 for the energy acceptor BChl-*a* in the baseplate protein in the outer membrane. The shifts in polarization angles between the two emission bands were distributed over all the possible values with a sharp peak around 90°, suggesting the perpendicular orientation between the transition dipoles of the fluorescence emission from the BChl-*c* aggregate and that from BChl-*a*. A simulation assuming a random orientation of chlorosomes reproduced the experimental results exactly. The analysis further indicated the appreciable contribution of the transition dipole of BChl-*c* that has an orientation perpendicular to the major polarization axis in each chlorosome. Small values of the degrees of polarization implied the BChl-*a* transition dipole to be somewhat tilted with respect to the normal of the cytoplasmic membrane to which chlorosomes are attached. These conclusions can be obtained only by observing the fluorescence of single chlorosomes.

Chlorosomes are unique and major photosynthetic antenna complexes in green sulfur and green filamentous bacteria (*1*, *2*). Chlorosomes show huge and oblong shapes with sizes of 100−200 nm × 30−50 nm × 12−18 nm depending on the species (*3*). The complex is attached to the inner surface of the cell cytoplasmic membranes and transfers light energy absorbed by bacteriochlorophyll (BChl)[1] *c*, *d*, or *e* in chlorosomes to the reaction center (RC) complex in the membrane. These pigments seem to self-aggregate to form supramolecules with little function of proteins. The supramolecular pigment aggregates are assumed to be surrounded by the envelope of the lipid monolayer (*2*). The pigment aggregates are known to transfer the excitation energy within a few tens of picoseconds to BChl-*a* in the baseplate protein, which is assumed to be buried in the envelope monolayer membrane of the chlorosome and is in contact with the cytoplasmic membrane. The energy is, then, transferred to the RC in the cytoplasmic membrane and used for the charge separation.

The freeze-fracture images of chlorosomes obtained by electron microscopy have revealed low-density tubular shapes, like "rods" inside chlorosomes (*4*−*6*). The rod diameter has been estimated to be 5 and 10 nm for the chlorosomes of green filamentous and green sulfur bacteria, respectively. The atomic-level structures of chlorosomal BChl self-aggregates have long been debated but not yet established (*7*−*11*). Holzwarth and Schaffner (*7*) proposed a model for the molecular architecture of chlorosomal rods based on a molecular modeling analysis. The model reproduced several experimental results, such as the rod diameters, absorption spectrum, circular dichroism, linear dichroism (LD) (*12*, *13*), and solid NMR data (*10*, *14*), quite reasonably. On the other hand, Pšenčík et al. (*8*, *9*) recently proposed a completely different lamellar-type structure for the pigment aggregates in chlorosomes on the basis of X-ray diffraction results.

Thus, the molecular architecture of BChl-*c* aggregates [designated (BChl-*c*)$_n$ hereafter] in a single chlorosome is still a matter of argument. Further examination is necessary to validate the fine calculations done so far on the basis of the rod model (*12*, *13*). Observation of polarization aniso-

† The work was supported in part by Grants-in-Aid for Scientific Research (17750010, 17029065, 15350107, and 18750158) and the 21st COE program for "the origin of the universe and matter" from the Japanese Ministry of Education, Science, Sports, and Culture (MEXT), and the Japan Society for the Promotion of Science. The work was also supported from the Academic Frontier Project for Private Universities (matching fund subsidy from MEXT, 2003−2007).

* To whom correspondence should be addressed. Telephone and fax: 81-52-789-2883. E-mail: yshibata@bio.phys.nagoya-u.ac.jp.

‡ Nagoya University.

§ Kinki University.

|| Ritsumeikan University.

[1] Abbreviations: BChl, bacteriochlorophyll; RC, reaction center; LD, linear dichroism; NMR, nuclear magnetic resonance; CCD, charge-coupled device; DP, degree of polarization; PS, phase shift; DP$_{single}$, degree of polarization of a single particle.

10.1021/bi0623072 CCC: $37.00
Published on Web 05/16/2007

tropy of a single molecule can be a powerful tool for shedding light on this interesting subject. Studies of single-molecule spectroscopy of the light-harvesting complex (LH2) of purple bacteria have indeed revealed the fine structure of the exciton states (*15*). Recently, we have demonstrated that the fluorescence spectroscopy of single chlorosomes gives new features of chlorosomes that are hidden by statistic averaging over an extremely large number of chlorosomes in the case of ordinary spectroscopies (*6*, *16*−*20*). Here, we report polarization anisotropy of single chlorosomes.

van Dorssen et al. (*21*) have demonstrated the (ensemble) LD measurement of chlorosomes isolated from a green filamentous bacterium, *Chloroflexus aurantiacus*, embedded in a squeezed polyacrylamide gel. Chlorosomes that were uniaxially aligned by squeezing and elongating the gel along one direction exhibited high anisotropies of the Q_y absorption bands of both (BChl-*c*)$_n$ and baseplate BChl-*a*. Their result and the following studies by several research groups (*22*−*25*) have validated the idea that the main transition dipole of the Q_y absorption band of (BChl-*c*)$_n$ is parallel to the long axis of whole chlorosome while that of the BChl-*a* band is almost perpendicular to it. On the basis of these results and electron microscope images, Mimuro et al. (*25*) have proposed a structural model of (BChl-*c*)$_n$ in which pigment molecules form rodlike aggregates with their Q_y transition dipoles parallel to the rod axis (*4*, *5*). In that model, the Q_y transition dipoles of (BChl-*c*)$_n$ and baseplate BChl-*a* were assumed to be situated almost parallel and perpendicular to the long axis of chlorosomes, respectively. The latter was assumed to be parallel to the normal of the cytoplasmic membrane. The angle between the two Q_y transition dipoles was estimated to be 87° (*25*).

In this study, we report that each single chlorosome purified from *Cfl. aurantiacus* shows clear and different fluorescence anisotropies of (BChl-*c*)$_n$ and BChl-*a* fluorescence bands. The results are compared with the results of the LD measurements for an ensemble of large amounts of chlorosome in the literature and lead us to draw new conclusions about the excited state of the chlorosome.

MATERIALS AND METHODS

The experimental procedure was essentially similar to that described previously (*18*, *20*). Chlorosomes were purified from *Cfl. aurantiacus* Ok-70-fl according to the method of Gerola and Olson (*26*) and suspended in a medium containing 50 mM Tris-HCl (pH 8.0) and 10 mM sodium dithionite. The suspension was mixed with 50% glycerol (v:v) to keep the transparency at a cryogenic temperature and sealed in a cavity between two quartz windows in a copper sample holder. The sample was set in a liquid-He flow-type cryostat (Microstat, Oxford Instruments, Eynsham, U.K.), and the fluorescence was measured at 13 ± 0.5 K. The measurement at 13 K immobilized chlorosomes in a frozen solvent and suppressed their damage by irradiation as described previously (*20*).

Fluorescence from a single chlorosome was measured according to previous studies (*18*, *20*) using a laser-scanning confocal microscope system (Nanofinder, Tokyo-Instruments, Tokyo, Japan) with a 458 nm excitation beam of an Ar^+ ion laser (5490ASL-00, Nippon Laser, Tokyo, Japan). The beam almost exclusively excited a Soret peak of (BChl-*c*)$_n$ and only slightly excited BChl-*a* in the baseplate protein. The fluorescence was passed through a dichroic mirror, a notch filter, and a long-pass filter and was then focused on the entrance slit of the monochromator, which was set at 200 μm to give sufficient signal intensity and high spatial resolution. This slit width gives a spectral resolution of ca. 4 nm. The fluorescence spectrum was measured using a cooled CCD detector (DU420-BV, Andor Technology, Belfast, U.K.).

To measure the polarization dependence of fluorescence from single chlorosomes, the polarizer was set in the light path between the monochromator and the dichroic mirror that separated the laser light and the fluorescence. The polarizer was rotated continuously with a speed of 20°/s, and the spectra were measured every 1 s; as a result, the intensity of fluorescence averaged over every 20° was collected. The excitation laser light was almost linearly polarized at the sample position, although it was slightly depolarized after passing through several optics. The degree of polarization of the excitation light typically took a value of ~0.9. The laser light is expected to be absorbed differently by each chlorosome depending on the relative orientation of the transition dipoles of the pigments with respect to the polarized laser beam and to emit different intensities of fluorescence.

Here we should stress that the direction of the electric field of the excitation light will not affect the direction of the polarization of the fluorescence from single chlorosomes. This is assumed because at cryogenic temperatures, the fluorescence is emitted from the excited singlet states of pigments at the lowest level in each chlorosome after the multiple excitation transfer steps that randomize the direction of the electric field of the original excitation light. Therefore, the detected polarization angle of the fluorescence of a single chlorosome will be affected only by the orientation of the lowest excited state, although the intensity itself is expected to vary with the orientation of each chlorosome with respect to the laser beam that determines the efficiency of excitation.

RESULTS AND DISCUSSION

Statistics of the Polarized Fluorescence of Single Chlorosomes. Panels A and B of Figure 1 show typical dependencies of the fluorescence spectra of single chlorosomes on the angle of the polarizer inserted into the detecting light path. The fluorescence was measured in the presence of sodium dithionite to eliminate quenching effects of intrinsic quenchers. Clear anisotropy was observed for fluorescence bands around 760 and 820 nm that are emitted from (BChl-*c*)$_n$ and BChl-*a* in the baseplate, respectively. This study, thus, clearly shows that chlorosomes in a random orientation (just dispersed in a medium and frozen to cryogenic temperatures) exhibit polarization anisotropy of fluorescence at the single-particle level similar to the case of a huge number of chlorosomes oriented in a squeezed gel (*21*−*25*). Smooth lines are the fitting curves calculated with respect to the wavenumber, ν, as a sum of skewed

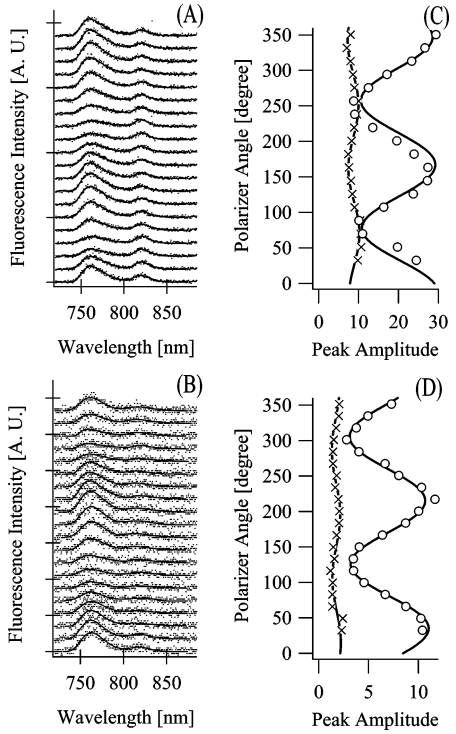

FIGURE 1: Dependence of the fluorescence spectra of single chlorosomes on the polarization angle of detection. (A and B) Fluorescence spectra (scattered dots) of single chlorosomes purified from *Cfl. aurantiacus* measured at different angles of the polarizer that was inserted in the monitoring light pass. Spectra are shifted vertically from the bottom to top at 20° increases in the angle of the polarizer. The smooth lines represent fitting curves calculated as the sum of skewed Gaussian functions (eq 1), as described in the text. (C and D) Dependence of the peak heights of the fluorescence bands of (BChl-*c*)$_n$ (○) and BChl-*a* (×) on the angle of the polarizer. The angle is set to be 0° at the position where excitation and detection polarizations are parallel. The solid and dotted lines are the fitting curves for the oscillation of the (BChl-*c*)$_n$ and BChl-*a* fluorescence peaks, respectively.

Gaussian function (*27*) expressed as

$$F(\nu) = \sum_{i=1}^{2} F_i \times \exp\left(-\ln 2 \times \left\{\frac{\ln[1 + 2b_i(\nu - \nu_{\max,i})/\Delta\nu_i]}{b_i}\right\}^2\right) \quad (1)$$

where F_i, $\nu_{\max,i}$, and $\Delta\nu_i$ are the height, peak wavenumber, and bandwidth of the ith component, respectively. b_i is the asymmetry parameter. When b is negative (positive), the model curve expresses an asymmetric shape with a gentler slope on the lower (higher) wavenumber side. When $b_i = 0$, the shape gives a symmetric Gaussian curve. The observed spectra are adequately fitted by two skewed Gaussian curves, which represent the short- and long-wavelength bands of (BChl-*c*)$_n$ and BChl-*a*, respectively. Typically, the asymmetry parameter b took the values of ca. −0.4 for the BChl-*c* band and ca. −0.2 for the more symmetric BChl-*a* band on average. These values are consistent with those previously estimated (*20*).

In panels C and D of Figure 1, the peak heights F of (BChl-*c*)$_n$ (○) and BChl-*a* (×) bands are plotted versus the polarizer angle. The polarizer angle was set to be 0° at the position where the orientations of the polarization of the excitation light and the analyzing polarizer are parallel to each other. F values exhibited oscillation with a period of 180°. Solid lines are the fitting curves expressed as an exponentially decaying cosine function

$$[y_0 + A\cos^2(\theta - \theta_0)]\exp\left(-\frac{\theta}{\tau}\right) \quad (2)$$

where θ, θ_0, A, and y_0 are the angle of the polarizer, the angle of the initial phase, the amplitude of oscillation, and the amplitude of the nonoscillating component, respectively. The decay time τ is introduced to compensate for the slight decrease in the fluorescence during the measurement, which is independent of the polarizer angle. The excitation laser power used in this study is sufficiently low to avoid severe degradation of single chlorosomes during the measurement at 13 K (*20*). The fluorescence intensity was sometimes weakened or intensified, probably due to slight temporal fluctuations in the alignment or focus of the excitation laser or in the chlorosome condition. These data were omitted in the statistics. In most cases, the fluctuation or degradation was negligible, as shown in Figure 1.

In Figure 1C, θ_0 was estimated to be 12° from the fluorescence maximum, while in Figure 1D, it was determined to be −35°. The low value of θ_0 near 0° shows almost parallel polarizations between the excitation light and the fluorescence emitted from this particular chlorosome. This is, however, not the evidence for the parallel orientations of the transition dipoles of the absorbing and emitting states, since the absorbing transition dipole is not always parallel to the electric field of the excitation light. It is noted that in this experiment, θ_0 took various values but its absolute value never exceeded 65°.

The intensities of (BChl-*c*)$_n$ and BChl-*a* bands oscillated differently. The majority of them oscillated in phases shifted by almost 90° with respect to each other (Figure 1C), while in some chlorosomes, they oscillated in similar phases, as shown in panel D. The oscillations in the almost 90°-shifted phases of (BChl-*c*)$_n$ and BChl-*a* fluorescence bands were also seen in panel A. We measured 51 single chlorosomes and found that the phase shifts were distributed over a wide range of angles from −45 to 130°. We also noticed that the ratio between the maximum and minimum fluorescence intensities, namely, the contrast of the oscillation, differs among single chlorosomes.

From the results of the fitting of the oscillation in fluorescence intensity to eq 2, we calculated the degree of polarization of a single chlorosome (DP_{single}) and the phase shift (PS) of the fluorescence of a single chlorosome as defined below:

$$DP_{single} \equiv \frac{F_{max} - F_{min}}{F_{max} + F_{min}} = \frac{A}{2y_0 + A} \quad (3)$$

$$PS = \theta_{c0} - \theta_{a0} \quad (4)$$

where F_{max} and F_{min} are the maximum and minimum fluorescence intensities during the oscillation, respectively. θ_{c0} and θ_{a0} are the initial phases of the oscillation for (BChl-*c*)$_n$ and BChl-*a* fluorescence bands, respectively. It should be noted here that DP_{single} is different from the ordinary definition of the degree of polarization (DP). We

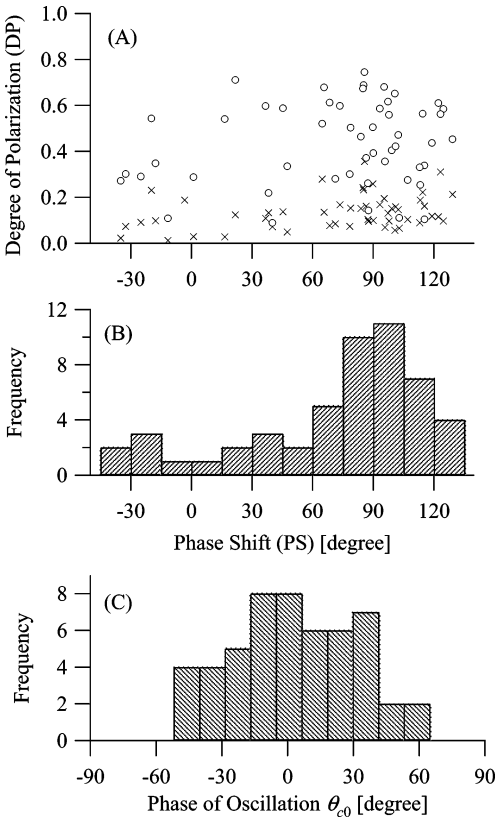

FIGURE 2: Degree of polarization, phase shift, and initial phase of (BChl-*c*)$_n$ fluorescence oscillation of single chlorosomes. (A) Values of DP$_{single}$ (degree of polarization in a single chlorosome) of the fluorescence from (BChl-*c*)$_n$ (○) and BChl-*a* (×). (B) Distribution of the PS (phase shift) value measured for 51 single chlorosomes plotted vs their PS values. (C) Distribution of the initial phase θ_0 of the oscillation in the (BChl-*c*)$_n$ fluorescence intensity.

calculated DP$_{single}$ using the values of the maximum and minimum fluorescence intensities in the oscillation, while the ordinary DP value is calculated using the values of the fluorescence intensities measured at polarization angles parallel and perpendicular to the polarization of the excitation light. In the case of the fluorescence from a single particle, the direction of fluorescence polarization is not related directly to that of the excitation light but totally depends on the orientation of the particle with respect to the direction of the analyzing polarizer. The direction of the excitation light affects only the efficiency of the excitation. DP$_{single}$ defined in eq 3 expresses how the emitted fluorescence is anisotropic but is not related to the relative angle between the polarizations of the excitation light and the fluorescence. DP$_{single}$, thus defined, becomes unity if all the transition dipole moments of emitting molecules (or excitonic states) in (BChl-*c*)$_n$ or BChl-*a* molecules in an observed single chlorosome are parallel to the detection angle. It becomes null if the emitting molecules inside a chlorosome are randomly oriented even if it is excited by linearly polarized light. PS corresponds to the angle between the projection vectors of the transition dipoles of emissions of (BChl-*c*)$_n$ and BChl-*a* to the plane perpendicular to the axis of an objective lens.

We estimated the values of DP$_{single}$ and PS for 51 single chlorosomes, as shown in Figure 2. Here, the DP$_{single}$ values of (BChl-*c*)$_n$ (○) and BChl-*a* (×) fluorescence bands for all 51 single chlorosomes are plotted against the PS values. No clear correlation was detected between PS and DP$_{single}$ in Figure 2A. The DP$_{single}$ of the (BChl-*c*)$_n$ fluorescence scattered over a range of 0−0.8 and never exceeded 0.8, while the DP$_{single}$ values for the BChl-*a* fluorescence had values of 0−0.3. The wide distribution of DP$_{single}$ values for both (BChl-*c*)$_n$ and BChl-*a*, shown in Figure 2A, can be available only via application of single-particle spectroscopy. The method enabled us to directly see the arrangement of fluorescence-emitting pigments in a single chlorosome that cannot be available by conventional techniques.

Histograms of the PS values are shown in Figure 2B. The distribution of PS exhibited a peak around 90°, suggesting an almost right angle between the transition dipoles of emitting states (the lowest excited state) of (BChl-*c*)$_n$ and BChl-*a*. The PS values were distributed over the whole region from −45 to 135°. Although small peaks at −22.5 and 37.5° might represent some structure in the distribution pattern, these peaks are still uncertain with the limited number of single chlorosomes inspected in this study. We, therefore, do not discuss them in this article. The reason for the wide distribution is discussed below.

Figure 2C shows the histogram of θ_{c0}, the initial phase of the fluorescence oscillation of (BChl-*c*)$_n$. The distribution of θ_{c0} has its maximum near 0°. This is an implication of nearly parallel orientations of polarizations between the absorbing and emitting states. The more precise mutual angle between the two polarization vectors will be estimated by the future measurements and analysis of the dependences of fluorescence intensity on the directions of polarizations of both the excitation light and the emitted fluorescence.

The pattern of the distribution of the θ_{c0} value is related to the sensitivity of our measurement system. If the sensitivity of the system is infinitely high, we will be able to measure even a chlorosome that has the absorbing transition dipole almost perpendicular to the direction of the polarization of excitation light. In this case, θ_{c0} will have any possible values. The definite θ_{c0} distribution shown in Figure 2C suggests that our measurement system can detect rather strong fluorescence emitted from only the chlorosomes whose absorbing transition dipoles are oriented nearly parallel to the polarization of the excitation light.

Simulation of the Polarized Fluorescence of Single Chlorosomes. We simulated the wide distributions of the DP$_{single}$ and PS values in Figure 2 by considering the random orientations of chlorosomes in a frozen solvent with the fixed mutual geometries of (BChl-*c*)$_n$ and BChl-*a*. The distributions obtained in the experiment were realized well (Figure 3) except for the subtle peaks around −22.5 and 37.5° by the simulation as follows. As shown in Figure 4A, the *z*-axis fixed in a single chlorosome is defined to be parallel to its long axis. The *x*- and *y*-axes are, then, defined to be parallel and perpendicular to the normal of the chlorosome envelope in contact with the cytoplasmic membrane, respectively. The distribution of the transition dipoles can be expressed by three principal dipole components along three principal axes perpendicular to each other.

According to the LD study of a squeezed chlorosome gel (*21*−*25*), the major component of the transition dipole of (BChl-*c*)$_n$ can be assumed to be almost parallel to the *z*-axis of the chlorosome. Although there has been no unambiguous information about the direction of the transition dipole of the lowest emitting state of the (BChl-*c*)$_n$ band at present, here we assumed as a working hypothesis that its major

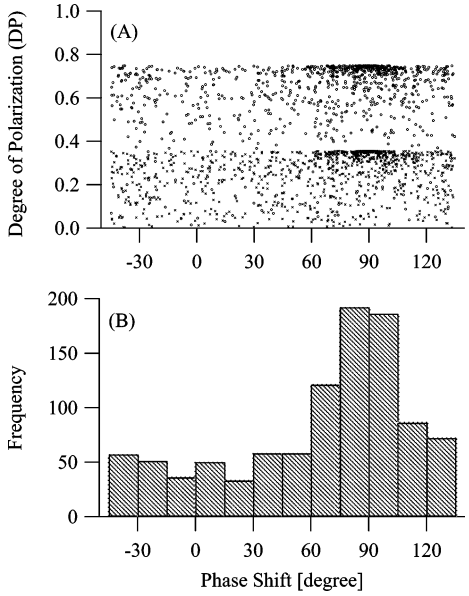

FIGURE 3: (A) Simulation of the DP values for the fluorescence of (BChl-*c*)$_n$ (○) and BChl-*a* (×) for 1000 randomly oriented chlorosomes based on the model described in the text. (B) Distribution of the simulated PS values.

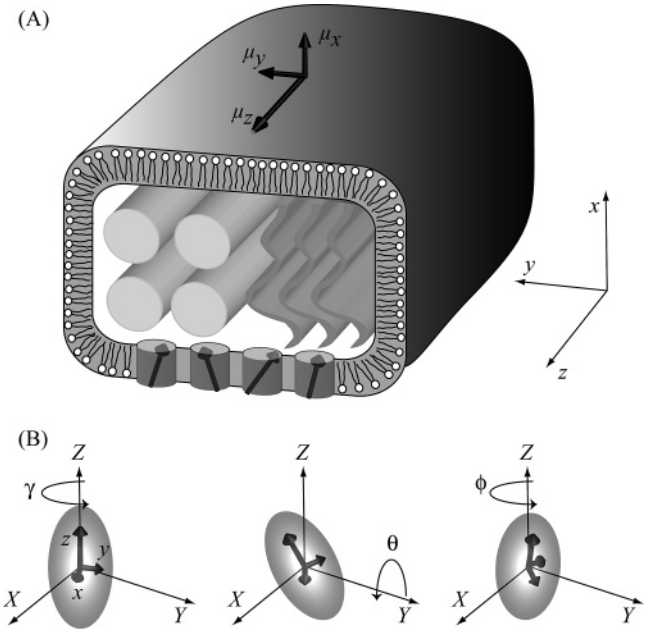

FIGURE 4: (A) Schematic description of the *x*-, *y*-, and *z*-axes fixed in a single chlorosome. A chlorosome is sectioned along the plane perpendicular to its long axis and is drawn according to Frigaard et al. (*28*). (BChl-*c*)$_n$ is shown in the rod model (left) by assuming its axis is parallel to the long axis of the chlorosome, and also in the lamellar model (right). The baseplate proteins are depicted as vertically aligned cylinders in the basal plain. The arrows in the baseplate represent the assumed Q_y transition dipole moments of BChl-*a* tilted at a constant angle from the *x*-axis according to the results in this study (see the text). (B) Definition of the orientation of a chlorosome with respect to the laboratory system. A chlorosome is drawn as an ellipsoid. The principal dipoles μ_x, μ_y, and μ_z for both (BChl-*c*)$_n$ and BChl-*a* are parallel to the *x*-, *y*-, and *z*-axes fixed in a chlorosome, which are shown as arrows within the chlorosome.

principal axis is parallel to the *z*-axis and designated the dipole component along the *z*-axis as $\boldsymbol{\mu}c_z$. This assumption, although in need of further validation, is consistent with the observation in Figure 2C, where the initial phase of the oscillation of (BChl-*c*)$_n$ fluorescence, θ_{c0}, is distributed around 0°. It is also compatible with the lamellar model proposed for the *Chlorobium tepidum* chlorosome, in which the Q_y transition dipole of all the pigment in the aggregate is assumed to be aligned parallel to the long axis of the chlorosome (*z*-axis) (*8*). According to the rod model, on the other hand, the direction of the transition dipole of the lowest exciton state will depend on the extent of the diagonal and off-diagonal disorder. The direction of the main transition dipole of the lowest level assumed in this study will be also realized by assuming a small extent of disorder in the rod model. The $|\boldsymbol{\mu}c_z|$ value was designated as μc_z. The other two principal dipole components were assumed to be parallel to *x*- and *y*-axes and designated as $\boldsymbol{\mu}c_x$ and $\boldsymbol{\mu}c_y$, respectively, as shown in Figure 4A. For the sake of simplicity, we here assume that the $|\boldsymbol{\mu}c_x|$ and $|\boldsymbol{\mu}c_y|$ values are the same and are expressed as $\mu c_x = \mu c_y = \mu c_{xy}$.

We define the *Z*-axis of the laboratory system to be parallel to the axis of the objective lens. If a chlorosome is oriented with its $\boldsymbol{\mu}c_z$ perpendicular to the *Z*-axis, the ratio of the minimum/maximum fluorescence intensities (F_{min}/F_{max}) becomes $(\mu c_{xy}/\mu c_z)^2$ and will give the highest value of DP_{single}. On the other hand, if $\boldsymbol{\mu}c_z$ is parallel to the *Z*-axis, the ratio will become $(\mu c_x/\mu c_y)^2$, which is here assumed to be unity and then yields a DP_{single} value of zero.

The low DP_{single} values of the BChl-*a* fluorescence of single chlorosomes may suggest a rather isotropic orientation distribution of the Q_y transition dipoles of BChl-*a* molecules in a single chlorosome, which can be expressed by the three principal dipole components, $\boldsymbol{\mu}a_x$, $\boldsymbol{\mu}a_y$, and $\boldsymbol{\mu}a_z$. The Q_y transition dipole of BChl-*a* was shown to be almost perpendicular to $\boldsymbol{\mu}c_z$ in the measurement of the squeezed gel (*21*−*25*). On the basis of this observation, we assume that the major Q_y transition dipole in BChl-*a*, $\boldsymbol{\mu}a_x$, is parallel to the *x*-axis in a single chlorosome and that $|\boldsymbol{\mu}a_y|$ and $|\boldsymbol{\mu}a_z|$ have the same value of μa_{yz}. Under these assumptions, the PS value will be 90° if both $\boldsymbol{\mu}c_z$ and $\boldsymbol{\mu}a_x$ are perpendicular to the *Z*-axis, while it will be 0° if both $\boldsymbol{\mu}c_z$ and $\boldsymbol{\mu}a_x$ are in the plane parallel to the *Z*-axis.

On the basis of the considerations given above, we simulated the DP_{single} and PS values by assuming certain values of four transition dipole components, μc_z, μc_{xy}, μa_x, and μa_{yz}, in randomly oriented single chlorosomes. The orientation of a chlorosome with respect to the laboratory system is schematically described in Figure 4B. We consider a chlorosome initially aligned to give *x*-, *y*-, and *z*-axes in parallel to *X*-, *Y*-, and *Z*-axes of the laboratory system, respectively. The arbitrary orientation of a chlorosome can then be expressed by rotating γ around the *Z*-axis, θ around the *Y*-axis, and ϕ around the *Z*-axis. The random distribution of the orientation of chlorosomes is expressed as being proportional to $\sin(\theta)$, which is reproduced from the generation of random numbers as

$$\gamma = 2\pi u,\ \phi = 2\pi v,\ \theta = \cos^{-1}(2w - 1) \qquad (5)$$

where *u*, *v*, and *w* are random numbers between 0 and 1. In Figure 3, we plot the DP values against the PS values that were simulated from the 1000 random numbers that were generated. The ratios of $\mu c_{xy}/\mu c_z$ and $\mu a_{yz}/\mu a_x$ could be inferred from the highest values of DP for the (BChl-*c*)$_n$ and BChl-*a* bands, respectively, in Figure 2. The distribution

detected in Figure 2 can be reproduced well with $\mu c_{xy}/\mu c_z$ and $\mu a_{yz}/\mu a_x$ values of 0.43 and 0.76, respectively.

The major dipole components of (BChl-*c*)$_n$- and BChl-*a*-emitting states are assumed a priori to be perpendicular to each other in the simulation described above. If the two dipole components exhibit a mutual angle significantly smaller than 90°, the distribution of PS values with a peak around 90° cannot be realized. Thus, this study clearly indicates the nearly perpendicular orientation between the transition dipoles of (BChl-*c*)$_n$- and BChl-*a*-emitting states at cryogenic temperatures. Although the mutual angle between the absorbing and emitting transition dipoles of (BChl-*c*)$_n$ at cryogenic temperatures has not yet been determined unambiguously, the θ_{c0} distribution around 0° suggests their nearly parallel orientations. The simulation further revealed high contributions of $\boldsymbol{\mu}c_x$ and $\boldsymbol{\mu}c_y$, which are perpendicular to the long axis of a chlorosome. The results in this study gave a high $\mu c_{xy}/\mu c_z$ value of 0.43 even at 13 K. These values seem to be useful in the examination of the relevance of the various structural models of pigment aggregates. There have been several molecular-scale structural models of rod architecture, and the detailed calculations of exciton states have been carried out on the basis of them. We are now estimating the extent of the diagonal and off-diagonal disorder in the model calculation to realize the $\mu c_{xy}/\mu c_z$ value obtained above. The results of the simulation presented here do not rely on the model structure of (BChl-*c*)$_n$ and also seem to be useful in the examination of the validity of the lamellar model, if the molecular-scale structural model may become available. The non-zero value of $\mu c_{xy}/\mu c_z$ seems also to be compatible with the lamellar model.

The value of $\mu a_{yz}/\mu a_x$ gives new information for the arrangement of BChl-*a* in the baseplate protein in a single chlorosome. Montano et al. (*29*) have isolated the CsmA protein from *Cfl. aurantiacus* and assigned it to the baseplate protein. The protein contained an average of 1.6 molecules of BChl-*a*. This implies that each CsmA binds either 1 or 2 molecules of BChl-*a*. The measurement of the CD spectrum has indicated that some BChl-*a* might exist as dimers in chlorosomes of green sulfur bacteria (*26*). If this is the case, the fluorescence at 13 K should be emitted from the terminal emitter at the lower excitonic state. The average number of BChl-*a* molecules per CsmA of 1.6 implies the fluorescence emission only from the one type of BChl-*a*. If the baseplate proteins are aligned to give the parallel orientation of dipoles of BChl-*a* in a single chlorosome, as expected from the periodic alignment of the baseplate aggregate (*5*), high DP_{single} and low $\mu a_{yz}/\mu a_x$ values are to be expected. However, we obtained a high value of 0.76 for $\mu a_{yz}/\mu a_x$. One possible way to explain this high value is that the Q_y transition dipole of BChl-*a* is tilted with an angle of β from the *x*-axis and rotates freely around the *x*-axis, as shown in Figure 4A. Here, the value of β is calculated to be 47° according to the relation $\tan(\beta)/\sqrt{2} = 0.76$. The factor of $1/\sqrt{2}$ reflects the random orientation of the baseplate proteins around the *x*-axis. The Q_y transition dipole of BChl-*a* in a baseplate protein is thus assumed to be tilted from the *x*-axis, but the major transition dipole of baseplate proteins seems to be located parallel to the *x*-axis on average due to its random orientation around the *x*-axis. The tilted transition dipole of the baseplate will affect the efficiency of energy transfer between (BChl-*c*)$_n$ and BChl-*a* in the core antenna complex in the cytoplasmic membrane. This type of orientation of the baseplate has not been obtained via a conventional LD study.

REFERENCES

1. Olson, J. M. (1998) Chlorophyll organization and function in green photosynthetic bacteria, *Photochem. Photobiol. 67*, 61−75.
2. Blankenship, R. E., Olson, J. M., and Miller, M. (1995) Antenna complexes from green photosynthetic bacteria, in *Anoxygenic Photosynthetic Bacteria* (Blankenship, R. E., Madigan, M. T., and Bauer, C. E., Eds.) pp 399−435, Kluwer Academic Publshers, Dordrecht, The Netherlands.
3. Sprague, S. G., and Varga, A. R. (1986) Photosynthetic membranes and light harvesting systems, in *Encyclopedia of Plant Physiology, Vol. 19* (Staehelin, L. A., and Arntzen, C. J., Eds.) pp 603−619, Springer-Verlag, Berlin.
4. Staehelin, L. A., Golecki, J. R., Fuller, R. C., and Drews, G. (1978) Visualization of supramolecular architecture of chlorosomes (*Chlorobium*-type vesicles) in freeze-fractured cells of *Chloroflexus aurantiacus*, *Arch. Microbiol. 119*, 269−277.
5. Staehelin, L. A., Golecki, J. R., and Drews, G. (1980) Supramolecular organization of chlorosomes (chlorobium vesicles) and of their membrane attachment sites in *Chlorobium limicola*, *Biochim. Biophys. Acta 589*, 30−45.
6. Saga, Y., and Tamiaki, H. (2006) Transmission electron microscopic study on supramolecular nanostructures of bacteriochlorophyll self-aggregates in chlorosomes of green photosynthetic bacteria, *J. Biosci. Bioeng. 102*, 118−123.
7. Holzwarth, A. R., and Schaffner, K. (1994) On the structure of bacteriochlorophyll molecular aggregates in the chlorosomes of green bacteria. A molecular modelling study, *Photosynth. Res. 41*, 225−233.
8. Pšenčík, J., Ikonen, T. P., Laurinmäki, P., Merckel, M. C., Butcher, S. J., Serimaa, R. E., and Tuma, R. (2004) Lamellar organization of pigments in chlorosomes, the light harvesting complexes of green photosynthetic bacteria, *Biophys. J. 87*, 1165−1172.
9. Pšenčík, J., Arellano, J. B., Ikonen, T. P., Borrego, C. M., Laurinmäki, P. A., Butcher, S. J., Serimaa, R. E., and Tuma, R. (2006) Internal structure of chlorosomes from brown-colored *Chlorobium* species and the role of carotenoids in their assembly, *Biophys. J. 91*, 1433−1440.
10. Umetsu, M. J., Hollander, G., Matysik, J., Wang, Z.-Y., Adschiri, T., Nozawa, T., and de Groot, H. J. M. (2004) Magic-angle spinning nuclear magnetic resonance under ultrahigh field reveals two forms of intermolecular interaction within CH_2Cl_2-treated (3^1R)-type bacteriochlorophyll *c* solid aggregate, *J. Phys. Chem. B 108*, 2726−2734.
11. Tamiaki, H., Shibata, R., and Mizoguchi, T. (2006) The 17-propionate function of (bacterio)chlorophylls: Biological implication of their long esterifying chains in photosynthetic systems, *Photochem. Photobiol. 83*, 152−162.
12. Prokhorenko, V. I., Steensgaard, D. B., and Holzwarth, A. R. (2000) Exciton dynamics in the chlorosomal antennae of the green bacteria *Chloroflexus aurantiacus* and *Chlorobium tepidum*, *Biophys. J. 79*, 2105−2120.
13. Prokhorenko, V. I., Steensgaard, D. B., and Holzwarth, A. R. (2003) Exciton theory for supramolecular chlorosomal aggregates: 1. Aggregate size dependence of the linear spectra, *Biophys. J. 85*, 3173−3186.
14. van Rossum, B.-J., Steensgaard, D. B., Mulder, F. M., Boender, G. J., Schaffner, K., Holzwarth, A. R., and de Groot, H. J. M. (2001) A refined model of the chlorosomal antenna of the green bacterium *Chlorobium tepidum* from proton chemical shift constraints obtained with high-field 2-D and 3-D MAS NMR dipolar correlation spectroscopy, *Biochemistry 40*, 1587−1595.
15. van Oijen, A. M., Ketelaars, M., Köhler, J., Aartsma, T. J., and Schmidt, J. (1999) Unraveling the electronic structure of individual photosynthetic pigment-protein complexes, *Science 285*, 400−402.
16. Saga, Y., Wazawa, T., Mizoguchi, T., Ishii, Y., Yanagida, T., and Tamiaki, H. (2002) Spectral heterogeneity in single light-harvesting chlorosomes from green sulfur photosynthetic bacterium *Chlorobium tepidum*, *Photochem. Photobiol. 75*, 433−436.
17. Saga, Y., Wazawa, T., Nakada, T., Ishii, Y., Yanagida, T., and Tamiaki, H. (2002) Fluorescence emission spectroscopy of single

light-harvesting complex from green filamentous photosynthetic bacteria, *J. Phys. Chem. B 106*, 1430−1433.
18. Saga, Y., Tamiaki, H., Shibata, Y., and Itoh, S. (2005) Excitation energy transfer in individual light-harvesting chlorosome from green photosynthetic bacterium *Chloroflexus aurantiacus* at cryogenic temperature, *Chem. Phys. Lett. 409*, 34−37.
19. Saga, Y., Wazawa, T., Ishii, Y., Yanagida, T., and Tamiaki, H. (2006) Single supramolecule spectroscopy of natural and alkaline-treated chlorosomes from green sulfur photosynthetic bacteria, *J. Nanosci. Nanotechnol. 6*, 1750−1757.
20. Shibata, Y., Saga, Y., Tamiaki, H., and Itoh, S. (2006) Low-temperature fluorescence from single chlorosomes, photosynthetic antenna complexes of green filamentous and sulfur bacteria, *Biophys. J. 91*, 3787−3796.
21. van Dorssen, R. J., Vasmel, H., and Amesz, J. (1986) Pigment organization and energy transfer in the green photosynthetic bacterium *Chloroflexus aurantiacus*, *Photosynth. Res. 9*, 33−45.
22. van Amerongen, H., Vasmel, H., and van Grondellle, R. (1988) Linear dichroism of chlorosomes from *Chloroflexus aurantiacus* in compressed gels and electric field, *Biophys. J. 54*, 65−76.
23. van Amerongen, H., van Haeringen, B., van Gurp, M., and van Grondellle, R. (1991) Polarized fluorescence measurements on ordered photosynthetic antenna complexes, *Biophys. J. 59*, 992−1001.
24. Matsuura, K., Hirota, M., Shimada, K., and Mimuro, M. (1993) Spectral forms and orientation of bacteriochlorophyll *c* and *a* in chlorosomes of the green photosynthetic bacterium *Chloroflexus aurantiacus*, *Photochem. Photobiol. 57*, 92−97.
25. Mimuro, M., Hirota, M., Nishimura, Y., Moriyama, T., Yamazaki, I., Shimada, K., and Matsuura, K. (1994) Molecular organization of bacteriochlorophyll in chlorosomes of the green photosynthetic bacterium *Chloroflexus aurantiacus*: Studies of fluorescence depolarization accompanied by energy transfer processes, *Photosynth. Res. 41*, 181−191.
26. Gerola, P. D., and Olson, J. M. (1986) A new bacteriochlorophyll *a*-protein complex associated with chlorosomes of green sulfur bacteria, *Biochim. Biophys. Acta 848*, 69−76.
27. Sevilla, J. M., Dominguez, M., Garcia-Blanco, F., and Blazquez, M. (1989) Resolution of absorption spectra, *Comput. Chem. 13*, 197−200.
28. Li, H., Frigaard, N.-U., and Bryant, D. A. (2006) Molecular contact for chlorosome envelope proteins revealed by cross-linking studies with chlorosomes from *Chlorobium tepidum*, *Biochemistry 45*, 9095−9103.
29. Montano, G. A., Wu, H. M., Lin, S., Brune, D. C., and Blankenship, R. E. (2003) Isolation and characterization of the B798 light-harvesting baseplate from the chlorosomes of *Chloroflexus aurantiacus*, *Biochemistry 42*, 10246−10251.

BI0623072